The Journal of Immunology

Analysis of the Neuroinflammatory Response to TLR7 Stimulation in the Brain: Comparison of Multiple TLR7 and/or TLR8 Agonists

Niranjan B. Butchi, Susan Pourciau, Min Du, Tim W. Morgan and Karin E. Peterson

J Immunol 2008; 180:7604-7612; ;
doi: 10.4049/jimmunol.180.11.7604
http://www.jimmunol.org/content/180/11/7604

The Journal of Immunology is published twice each month by
The American Association of Immunologists, Inc.,
1451 Rockville Pike, Suite 650, Rockville, MD 20852

Print ISSN: 0022-1767 Online ISSN: 1550-6606.

Analysis of the Neuroinflammatory Response to TLR7 Stimulation in the Brain: Comparison of Multiple TLR7 and/or TLR8 Agonists[1]

Niranjan B. Butchi, Susan Pourciau, Min Du, Tim W. Morgan, and Karin E. Peterson[2]

Activation of astrocytes and microglia and the production of proinflammatory cytokines and chemokines are often associated with virus infection in the CNS as well as a number of neurological diseases of unknown etiology. These inflammatory responses may be initiated by recognition of pathogen-associated molecular patterns (PAMPs) that stimulate TLRs. TLR7 and TLR8 were identified as eliciting antiviral effects when stimulated by viral ssRNA. In the present study, we examined the potential of TLR7 and/or TLR8 agonists to induce glial activation and neuroinflammation in the CNS by intracerebroventricular inoculation of TLR7 and/or TLR8 agonists in newborn mice. The TLR7 agonist imiquimod induced astrocyte activation and up-regulation of proinflammatory cytokines and chemokines, including IFN-β, TNF, CCL2, and CXCL10. However, these responses were only of short duration when compared with responses induced by the TLR4 agonist LPS. Interestingly, some of the TLR7 and/or TLR8 agonists differed in their ability to activate glial cells as evidenced by their ability to induce cytokine and chemokine expression both in vivo and in vitro. Thus, TLR7 stimulation can induce neuroinflammatory responses in the brain, but individual TLR7 agonists may differ in their ability to stimulate cells of the CNS. ***The Journal of Immunology,*** **2008, 180: 7604–7612.**

Neuroinflammation, including astrogliosis and production of proinflammatory cytokines and chemokines, is a common finding following viral, bacterial, and parasitic infections of the CNS in both children and adults (1–9). Neuroinflammatory responses are also observed in autism, Alzheimer's disease, and other neurological diseases of unknown etiology (10–14). The neuroinflammatory response may be a common mechanism of pathogenesis leading to neuronal damage and long-term neurological disorders (15–18).

The initiation of inflammation is often associated with the recognition of pathogen-associated molecular patterns (PAMPs),[3] the repeated structural motifs that are unique to microorganisms (19–21). These PAMPs are recognized by transmembrane-bound TLRs as well as cytoplasmic or mitochondrial-associated pattern recognition receptors (PRRs) (19–21). There are at least 11 identified TLRs in humans and 12 TLRs in mice (22). Multiple TLRs are up-regulated in the CNS in response to pathogen infection (23–26). Of these receptors, several have been shown to contribute to neuroinflammatory responses and pathogenesis including TLR2, TLR3, TLR4, and TLR9 (27–33). Intracerebroventricular (icv) administration of agonists for either TLR4 or TLR9 induced strong neuroinflammatory responses and damage in the CNS (27, 34).

Two other TLRs that may play an important role in initiating innate immune responses in the CNS are TLR7 and TLR8. These receptors were originally identified as eliciting antiviral effects when stimulated by the family of guanosine-based imidazoquinoline compounds (35, 36) which includes imiquimod, loxoribine, and R-848. More recent studies identified the natural PAMP of TLR7 and TLR8 to be guanidine-uridine-rich ssRNA from viruses, suggesting that these receptors may be important modulators of the immune response to certain neurotropic viruses such as flaviviruses, paramyxoviruses, rhabdoviruses, and retroviruses. However, there remains a lack of basic understanding of the neuroinflammatory properties of TLR7 and TLR8.

Functional differences between mouse TLR7 and TLR8 have not been described; however, TLR7-deficient mice do not respond to imiquimod, R-848, or viral ssRNA. Furthermore, vesicular stomatitis virus and influenza A-induced IFN-α responses are suppressed in TLR7$^{-/-}$ mice (37, 38). This suggested that murine TLR8 may be biologically inactive in mice (35, 39). However, recent studies have demonstrated that murine TLR8, but not TLR7, is expressed on neurons in utero and in the first 2 wk after birth in the neonatal brain (40). Stimulation of neurons with TLR7/8 agonists induced caspase 3 activation and inhibited dendrite growth, suggesting that TLR8 may be functional in neonates and serves an important role in brain development (40).

In the present study, we analyzed the downstream responses to TLR7 and/or TLR8 stimulation in the developing brain. For this, we administered different TLR7/8 agonists by icv inoculation in newborn mice and analyzed the neuroinflammatory responses within the CNS. These results revealed that TLR7/8 agonists differed in their ability to induce neuroinflammation. The agonists that did induce neuroinflammatory responses induced pronounced activation of astrocytes and the production of chemokines by several cell types in the CNS.

Department of Pathobiological Sciences, School of Veterinary Medicine, Louisiana State University, Baton Rouge, LA 70803

Received for publication January 31, 2008. Accepted for publication March 20, 2008.

The costs of publication of this article were defrayed in part by the payment of page charges. This article must therefore be hereby marked *advertisement* in accordance with 18 U.S.C. Section 1734 solely to indicate this fact.

[1] This work was supported by National Institutes of Health Grant K22AI57118-2 and National Center for Research Resources Grant IP20RR020159.

[2] Address correspondence and reprint requests to Dr. Karin Peterson, Department of Pathobiological Sciences, School of Veterinary Medicine, Louisiana State University, Baton Rouge, LA 70803. E-mail address: kpeterson@vetmed.lsu.edu

[3] Abbreviations used in this paper: PAMP, pathogen-associated molecular pattern; CT, critical threshold; GFAP, glial fibrillary acidic protein; icv, intracerebroventricular; PRR, pathogen recognition receptor; DIG, digoxigenin; hpi, hours postinfection; hpi, hours postinoculation; IP-10, IFN-γ-inducible protein 10.

Table I. *Primers used for real-time RT-PCR analysis*

Common Name	NCBI[a] Gene Symbol and Identification No.	Forward Primer	Reverse Primer
CD3 Ag, ϵ polypeptide	Cd3ϵ: 12501	GAGCACCCTGCTACTCCTTG	TGAGCAGCCTGATTCTTTCA
Chemokine ligand 2, MCP-1	*Ccl2:* 20296	TCCCAATGAGTAGGCTGGAG	CCTCTCTCTTGAGCTTGGTGA
Chemokine ligand 10, IP-10	*Cxcl10:* 15945	CAGTGAGAATGAGGGCCATAGG	CTCAACACGTGGGCAGGAT
F4/80	*Emr1:* 13733	TTACGATGGAATTCTCCTTGTATATCA	CACAGCAGGAAGGTGGCTATG
GAPDH	*Gapdh:* 407972	TGCACCACCAACTGCTTAGC	TGGATGCAGGGATGATGTTC
GFAP	*Gfap:* 14580	CGTTTCTCCTTGTCTCGAATGAC	TCGCCCGTGTCTCCTTGA
IFN-β	*Ifnb1:* 15977	AGCACTGGGTGGAATGAGAC	TCCCACGTCAATCTTTCCTC
ICAM-1, CD54	*Icam-1:* 15894	AGGGCTGGCATTGTTCTCTA	CTTCAGAGGCAGGAAACAGG
TNF	*Tnf:* 21926	CCACCACGCTCTTCTGTCTAC	GAGGGTCTGGGCCATAGAA

[a] NCBI, National Center for Biotechnology Information.

Materials and Methods

Mice

Inbred Rocky Mountain White (IRW) mice at 48 h after birth were used for the present study. TLR7-deficient C57BL/6 mice (35) were provided by S. Akira (Osaka University, Osaka, Japan) and were backcrossed with IRW mice for 10 generations. Since the *Tlr7* gene is located on the X chromosome, male mice are either homozygous negative or homozygous positive for the *Tlr7* gene. TLR7-deficient male mice were crossed with TLR7 heterozygous female mice generating litters consisting of $Tlr7^{+/-}$ females, $Tlr7^{+}$ males, $Tlr7^{-/-}$ females, and $Tlr7^{-}$ males; with ~50% *Tlr7* positive (+/− or +) and 50% *Tlr7* negative ($^{-/-}$ or −). All of the animal procedures were conducted in accord with the Louisiana State University Animal Care and Use Committee guidelines.

Agonists of TLR4, TLR7, and TLR8

The TLR7 and/or TLR8 agonists, imiquimod (R837), loxoribine, 3M002 (CL075), CL087, and CL097 as well as the TLR4 agonist LPS were purchased from InvivoGen (35, 36, 41–44). All of the agonists were suspended in endotoxin-free water, aliquoted, and stored at −20°C until use. Just before use, agonists were diluted in endotoxin-free 1× PBS/0.2% trypan blue. The vehicle control, 0.2% trypan blue in PBS, was used for mock inoculations.

Intracerebroventricular inoculations of newborn mice

Mice, at ~48 h after birth, were anesthetized by hypothermia, and 10 μl (5 μl/hemisphere) of the appropriate TLR agonist or vehicle control was inoculated into the lateral ventricles using a 33-gauge needle and a Hamilton syringe according to a previously established protocol (45, 46). Correct ventricular inoculation was confirmed by observing trypan blue staining in the ventricles (45, 46). Mice were inoculated icv with either 2 μg of LPS, 50 μg (200 nmol) of imiquimod, or 10 μl of vehicle control (0.2% trypan blue in PBS). For the dose curve analysis, imiquimod was used at 20, 100, 200, or 500 nmol/mouse. The neuroinflammatory responses to imiquimod at the 100-nmol dosage were compared with the responses induced by other TLR7/8 agonists: loxoribine, 3M002 (CL075), CL087, and CL097 at a 100-nmol dosage.

Preparation of brain tissue for histological and molecular analysis

Animals inoculated icv with TLR7 or TLR4 agonists or vehicle control were anesthetized by deep inhalation anesthesia followed by axillary incision and cervical dislocation at the specified time points or at the end of the experimental protocol. Brains were removed and immediately cut into two halves by mid-sagittal dissection, snap frozen in liquid nitrogen, and stored at −80°C for molecular analysis. One half was used for RNA extraction and the other half was used for multiplex analysis of cytokine and chemokine production. Brains removed from the mice inoculated for in situ hybridization and/or immunohistochemistry were divided into four coronal sections using a brain matrix and fixed in 10% neutral-buffered formalin for 48 h before processing for histological analysis. Tissues were embedded in paraffin, cut in 4-μm sections, adhered to coated microscope slides, and stained with H&E using an automated histological stainer. Stained sections were blindly graded for inflammatory changes, neural/glial degeneration and necrosis by a veterinary pathologist.

RNA extraction

Total RNA from the brain tissue was isolated using TRIzol reagent (Invitrogen), treated with DNase (Ambion) for 30 min at 37°C, and purified over RNA cleanup columns (Zymo Research) before use. RNA samples were converted to cDNA using an iScript reverse transcription kit (Bio-Rad) according to the manufacturer's instructions. Before analysis by real-time PCR, following the reverse transcriptase reaction, samples were diluted 5-fold in RNase-free water for use in real-time PCR.

Analysis of mRNA expression by real-time PCR

The primers to detect *Cd3ε, Ccl2, Cxcl10, F4/80, Gfap, Icam-1, Ifnb1, and Tnf* cDNA were designed using Primer3 software (47), with a melting temperature of 60°C for all primers (Table I). All primer pairs were confirmed to be specific for the gene of interest, and no homology to other genes was detected when the primers were blasted against the National Center for Biotechnology Information database. A cDNA pool produced from mRNA from a macrophage cell line, an astroglia cell line, brain, and spleen tissue was used to analyze the specificity of primers. SYBR Green dye with ROX (Bio-Rad) was used for measurement of real-time PCR amplification. All samples were run in triplicate on a 384-well plate using a 7900 Applied Biosystems PRISM instrument with an automatic set baseline and a manual set critical threshold (CT) of 0.19, which intersects the mid-log phase of curves for all of the PCR pairs. The dissociation curves were used to confirm amplification of a single product for each primer pair per sample. A known positive control sample was run for the corresponding gene on all assays. RNA that did not undergo reverse transcription (DNA contamination control) and water were used as negative controls. Data for each sample were initially calculated as the percent difference in C_T value ($\Delta C_T = C_T$ *Gapdh* $- C_T$ gene of interest). The mean percent *Gapdh* values of mock samples for each time point were calculated and used to generate fold changes relative to mock expression for each group at each time point.

Multiplex analysis of cytokine and chemokine proteins

To generate tissue homogenates for analysis by multiplex bead array, brain samples were weighed and then homogenized in 200 μl of Bio-plex cell lysis solution (Bio-Rad) containing complete mini-protease inhibitors (Roche Applied Science) and 2 mM PMSF (Sigma-Aldrich). Samples were homogenized using Kontes disposable pellet pestles (Fisher Scientific) and volumes were adjusted to 1 ml/200 mg of tissue with lysis buffer. Cellular debris was removed by centrifugation at 4500 × *g* for 15 min at 4°C. Samples were analyzed for cytokine and chemokine protein expression using a BioSource 20plex assay (Invitrogen) on a Luminex 100 instrument (Bio-Rad) per the manufacturer's instructions. Samples were calculated as pg/ml using a standard curve from in-plate standards and subsequently converted to fg/mg brain tissue. For the majority of the positive samples (e.g., cytokine and chemokines at 12 h after imiquimod stimulation), the pg/ml concentration value was in the linear part of the standard curve.

In situ hybridization analysis

Due to the secreted nature of cytokines and chemokines, it can be difficult to detect the expression of these proteins or to determine their cellular source. In situ hybridization detects mRNA expression inside individual cells, thereby allowing for the detection of the cellular source of gene expression (48). In brief, dewaxed and rehydrated tissue sections adhered to glass slides were fixed in 4% paraformaldehyde followed by denaturation of proteins using 200 mM HCl. The sections were then incubated with 10 μg/ml proteinase K for 20 min. Sections were then dehydrated, incubated in chloroform, and then rehydrated. The sections were then incubated in 2× SSC buffer (Invitrogen), followed by incubation with hybridization buffer (10% dextran sulfate, 0.01% sheared salmon sperm DNA, 0.02% SDS, and 50% formamide in 1× SSC) at 56°C for 1–4 h. At the end of the incubation, digoxigenin (DIG)-labeled RNA antisense or

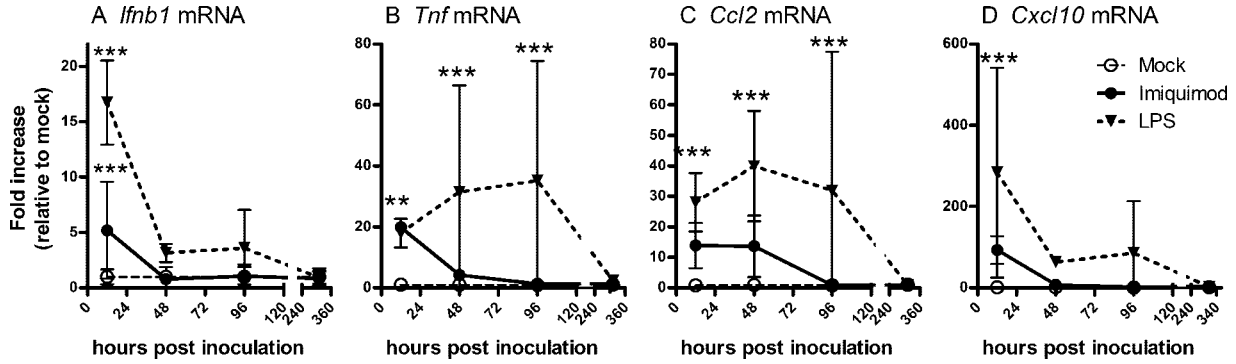

FIGURE 1. Induction of neuroinflammatory responses (*A–D*) following imiquimod or LPS inoculation in the brain. Mice at 48 h of age were inoculated by icv injection with 2 μg of LPS, 50 μg of imiquimod, or 10 μl of vehicle control (0.2% trypan blue in PBS). Brain tissues were removed at 12, 48, 96, or 312 hpi and snap frozen for RNA or protein analysis as described. RNA samples were processed for real-time quantitative RT-PCR analysis and values were calculated relative to expression of *Gapdh* controls. Data are presented as the fold induction of each gene of interest relative to mock-infected controls. Mock expression levels were calculated as the mean of six animals per time point. Data are the mean ± SD of three to seven mice per group per time point and represent the combined data from two independent experiments. Statistical analysis was completed by two-way ANOVA using Bonferroni's post test. **, $p < 0.01$ and ***, $p < 0.001$.

sense probes were added to the sections, covered with hybridization coverslips, and incubated overnight at 56°C. The slides were incubated in 2× SSC to remove the coverslips, followed by incubation in 50% formamide in 1× SSC for 60 min. Sections were incubated in blocking buffer (10× blocking buffer diluted in 1× maleic acid solution; Roche Biochemicals) and then incubated in a 1/100 dilution of alkaline phosphatase-conjugated anti-DIG Ab (Roche Molecular Biochemicals). The slides were then washed in blocking buffer, washed in 1× TBS, and incubated in detection buffer (0.1 M Tris-HCl, pH 8.2). The slides were then incubated in Fast Red solution (5-mg Fast Red tablet in 2 ml of 0.1 M Tris-HCl (pH 8.2); Biomedia) using gasket coverslips (Grace Biolabs) until color developed in the slides from treated animals. No staining was observed in mock controls or with nonspecific probes.

Immunohistochemistry analysis of in situ sections

When sufficient color was developed by in situ hybridization, gasket coverslips were removed and the slides were washed in 1× PBS. The sections were blocked in normal donkey serum blocking solution (PBS containing 2% donkey serum, 1% BSA, 0.1% cold fish skin gelatin, 0.1% Triton X-100, and 0.05% Tween 20) at 37°C for 60 min and incubated overnight at 4°C with polyclonal rabbit anti-glial fibrillary acidic protein (GFAP) Ab (DakoCytomation) in normal donkey serum blocking solution. Following two washes of 10 min in PBS, goat anti-rabbit IgG Ab labeled with HRP conjugate (Invitrogen) was applied and incubated at room temperature for at least 30 min. Slides were washed twice in PBS and incubated in metal-enhanced diaminobenzidine (Pierce). After sufficient color development, slides were washed twice in PBS, counterstained with hematoxylin, and covered with a glass coverslip using aqueous mounting medium (Lerner Laboratories).

TLR7 protein expression in astrocytes (C8D1A) and macrophages (RAW264.7) by flow cytometric analysis

RAW264.7 (ATCC TIB-71) and C8D1A (ATCC CRL-2541) were obtained from American Type Culture Collection and maintained according to American Type Culture Collection guidelines. Semiconfluent cultures of C8D1A and RAW264.7 cells were analyzed for TLR7 protein expression by intracellular staining. In short, cells were gently scraped off the plate, washed in PBS, and fixed for 20 min in 2% paraformaldehyde. Cells were permeabilized with 0.1% saponin in PBS (pH 7.0) and incubated with primary Abs, either polyclonal rabbit anti-bovine GFAP (DakoCytomation) or polyclonal rabbit anti-mouse TLR7 (Invitrogen) for 30 min at room temperature. Cells were washed twice with 0.1% saponin in PBS and incubated with Alexa Fluor 488-conjugated goat anti-rabbit IgG (Molecular Probes) for 30 min at room temperature in the dark. Cells were washed twice with 0.1% saponin in PBS, resuspended in PBS, and analyzed on a FACSAria flow cytometer (BD Biosciences) using FACSDiva software (BD Biosciences). Data analysis was performed using FlowJo software (Tree Star).

Stimulation of astrocytes and macrophages in vitro with TLR7 agonists, imiquimod, and loxoribine

Semiconfluent cultures of C8D1A astrocyte cells or RAW264.7 cells were seeded into 6-well plates and stimulated with imiquimod or loxoribine at 100 μM in 1 ml. Astrocyte cells were stimulated with imiquimod, loxoribine, or medium alone for 6, 12, 24, or 48 h in triplicate wells for each time point. Astrocyte cells were lysed within the well at specified time points and total RNA was extracted from the cells using a mini- RNA isolation kit (Zymo Research) according to the manufacturer's instructions.

Statistical analysis

All of the statistical analysis was performed using Prism software (GraphPad) and is described in the figure legends.

Results

Intracerebroventricular inoculation of TLR7 agonist induces a pronounced neuroinflammatory response in CNS

The first week after birth, the development of the neonatal mouse brain corresponds to the late second and early third trimester development of a human brain in terms of limbic and cortex development (49). The first few days after birth in the mouse are ideal for icv inoculations due to ease of inoculation and the ability to readily confirm inoculation in lateral ventricles. We examined the ability of TLR7 stimulation at this time point to induce neuroinflammatory responses using the TLR7 agonist imiquimod. We compared these responses to stimulation with the TLR4 agonist LPS which is known to induce severe neuroinflammation and damage to the neonatal brain (50). In addition, the comparison between TLR7 and TLR4 allows us to analyze the predicted differences in response between an intracellular PRR that recognizes viral products and extracellular PRR that primarily recognizes bacterial surface components.

Administration of the TLR7 agonist imiquimod induced a pronounced neuroinflammatory response in the brain at 12 h after inoculation with the up-regulation of mRNA for *Ifnb1* (IFN-β), *Tnf* (TNF), *Ccl2* (MCP-1), and *Cxcl10* (IFN-γ-inducible protein 10 (IP-10)) (Fig. 1), cytokines, and chemokines commonly associated with virus-induced neuroinflammation (51–53). In most cases, imiquimod-induced mRNA expression returned to basal levels by 48 h after stimulation, suggesting a short-term response. In contrast, LPS stimulation generally induced a longer term response with *Ccl2* and *Tnf* mRNA expression still significantly up-regulated at 96 h after inoculation (Fig. 1). The increase in cytokine and

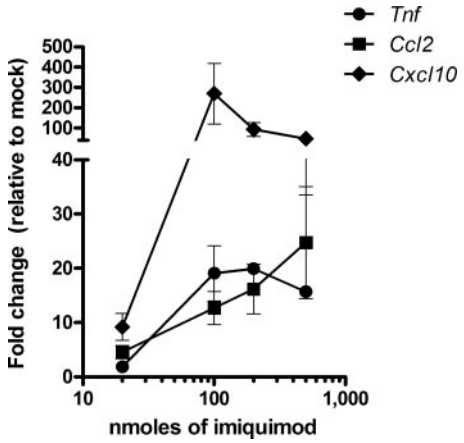

FIGURE 2. Cytokine response to imiquimod is dose dependent. Mice were treated as described in Fig. 1, but using varying concentrations of imiquimod in 10 μl of PBS/0.2% trypan blue. At 12 hpi, brain tissue was removed and processed for RNA. Samples were analyzed as described in Fig. 1. Data are the mean ± SD of three to seven mice per group and represent the combined data from two independent experiments.

chemokine expression did not correlate with any obvious clinical symptoms in the mice following icv inoculation with either LPS or imiquimod.

Optimal dose for TLR7-mediated inflammation

The ability of TLR7 to stimulate innate immune responses in the neonatal brain may be dose dependent. Imiquimod was administered at 20, 100, 200, and 500 nmol/mouse. No dose above 500 nmol was administered due to insolubility of the agonist. One hundred to 200 nmol of imiquimod was optimal for eliciting neuroinflammatory responses in the CNS at 12 h after inoculation, as demonstrated by up-regulation of mRNA for multiple cytokines such as *Tnf, Ccl2*, and *Cxcl10* (Fig. 2). Imiquimod at the 20-nmol dose did not stimulate any neuroinflammatory response, whereas 500 nmol of imiquimod induced higher responses for some cytokines and chemokines, but not others (Fig. 2).

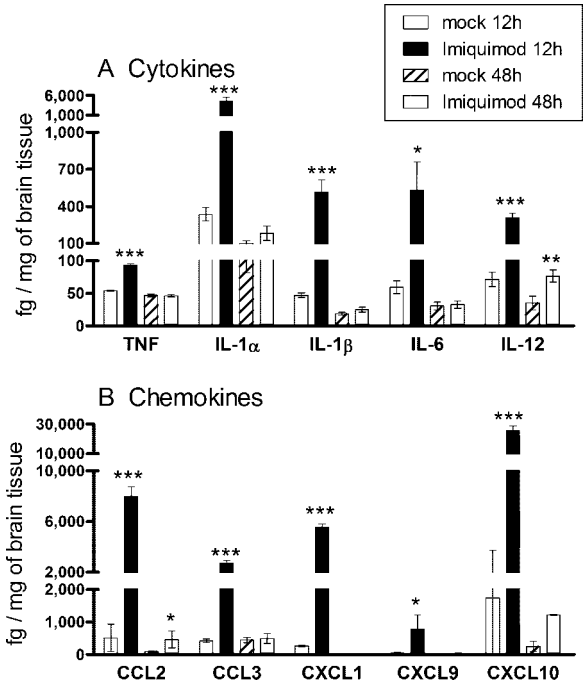

FIGURE 3. Increased protein expression of proinflammatory cytokines (*A*) and chemokines (*B*) in the CNS following stimulation with imiquimod. Mice were inoculated as described in Fig. 1 and tissues were removed at 12 or 48 hpi. One half of the sagitally divided brain was homogenized in lysis buffer containing protease inhibitors and analyzed for protein expression using a BioSource 20-plex bead array on a Bioplex Luminex system. Samples were calculated as pg/ml using a standard curve from in-plate standards and subsequently converted to fg/mg brain tissue. Data are the mean ± SD of three mice per group. Statistical analysis was completed by one-way ANOVA with Newman-Keuls post test. *, $p < 0.05$; **, $p < 0.01$; and ***, $p < 0.001$.

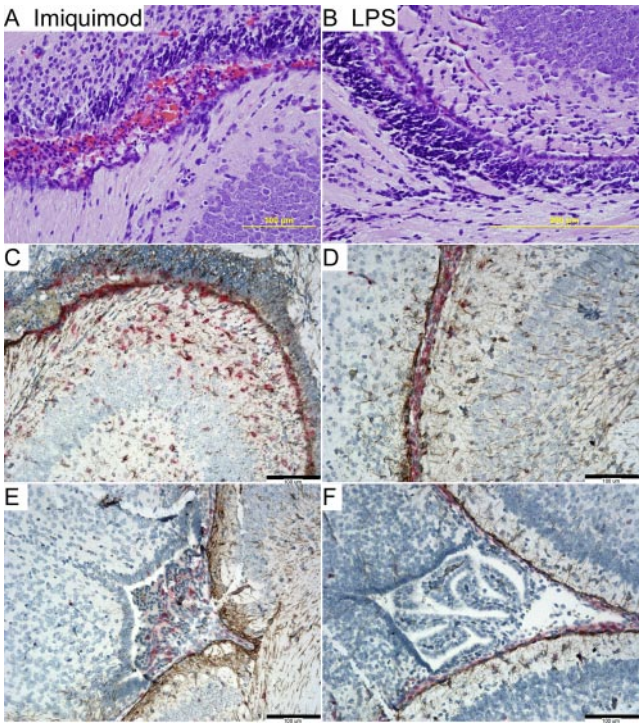

FIGURE 4. Comparison between imiquimod- and LPS-treated mice. *A* and *B,* H&E- stained mid-coronal sections of brain tissue from imiquimod- (*A*) and LPS-treated (*B*) mice at 12 hpi. Both images are of lateral ventricles and are representative of the three mice in each group. The imiquimod-treated mice have increased numbers of neutrophils, lymphocytes, and erythrocytes within the lateral ventricles (suppurative ventriculitis) (*A*) as compared with the LPS-treated mice, which have no appreciable inflammatory infiltrates (*B*). *C–F,* Analysis of brain tissue sections from imiquimod- (*C* and *E*) and LPS-treated (*D* and *F*) mice at 12 hpi for *Ccl2*-mRNA-expressing cells (bright red stain). *Ccl2* mRNA was detected using DIG-labeled RNA antisense probes and stained with Fast Red substrate. Cells were then stained with anti-goat GFAP Ab, followed by secondary Abs labeled with Alexa Fluor 488 and metal-enhanced diaminobenzidine (brown stain). *C* and *D,* Location of *Ccl2*-positive cells varies dramatically between imiquimod- (*C*) and LPS-treated (*D*) mice. Images are of same region and from same mice as in *A* and *B*. *E* and *F, Ccl2*-positive cells were also detected in the choroid plexus of imiquimod- (*E*) but not LPS-treated (*F*) mice. All images were taken with a digital camera attached to an Olympus scope. Scale bar is shown for all images: 100 μm (*A*, *C–F*), 200 μm (*B*). Data are representative of two separate experiments. Nonspecific RNA probes and no- primary Ab controls were used as controls for *C–F*.

Analysis of cytokines and chemokines induced by imiquimod

Multiplex bead assays were performed to determine which cytokines and chemokines were up-regulated by stimulation of TLR7. Proinflammatory cytokines TNF, IL-1α, IL-1β, IL-6, and IL-12 and chemokines CCL2, CCL3 (MIP-1α), CXCL1 (neutrophil-activating protein 3/KC), CXCL9 (monokine induced by γ IFN), and CXCL10 were up-regulated in the CNS following stimulation with imiquimod at 12 hours postinoculation (hpi; Fig. 3). By 48 hpi,

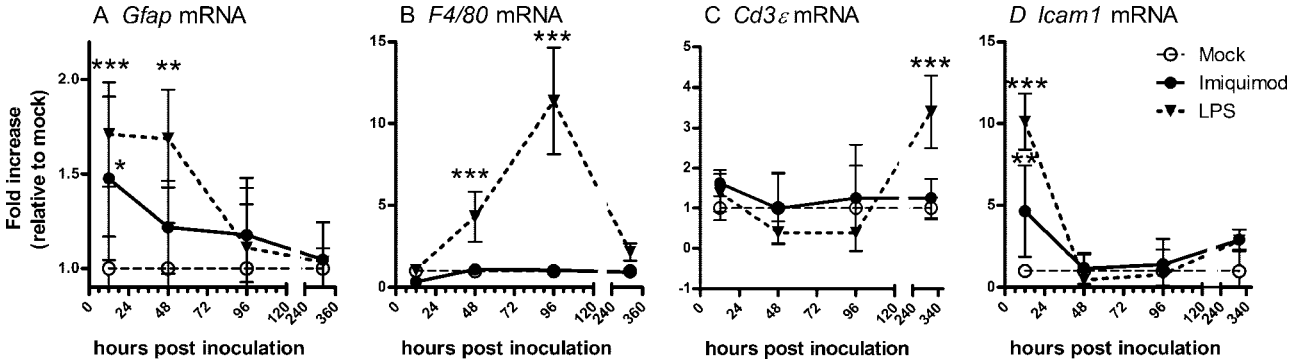

FIGURE 5. Kinetics of cellular responses (*A–D*) in the CNS following imiquimod or LPS inoculation in the neonatal brain. Brain tissues at 12, 48, 96, or 312 hpi were processed for real-time RT-PCR analysis using primers specific for *Gfap* (*A*), *F4/80* (*B*), *Cd3e* (*C*), and *Icam-1* (*D*) mRNA. Values calculated were relative to the expression of *Gapdh* controls. Data are analyzed as described in Fig. 1. Data are the mean ± SD of three to seven mice per group per time point and represent the combined data from two independent experiments. Statistical analysis was completed by two-way ANOVA using Bonferroni;s post test. **, $p < 0.01$ and ***, $p < 0.001$.

only IL-12, CCL2, CCL3, and CXCL9 remained elevated compared with mock controls (Fig. 3). Imiquimod administration did not induce the up-regulation of GM-CSF, IFN-γ, IL-5, IL-10, IL-13, or IL-17 at either time point (data not shown). LPS administration induced similar cytokines and chemokines to imiquimod, but with the additional up-regulation of IL-2 and IL-13 (data not shown). The increase of cytokine and chemokine production was substantially higher in the LPS-inoculated mice for almost all cytokines and chemokines, the exception being CXCL1 (data not shown).

Cellular responses in the CNS following TLR7 agonist administration

Since 12 hpi was the peak time for cytokine mRNA and protein production, we examined tissue samples from this time point for histological changes. All mice including mock controls had minimal to mild meningitis, characterized by infiltration of the meninges by variable numbers of neutrophils and lymphocytes. The cause of the minimal to mild meningitis in all mice is uncertain, but may be in response to the icv needle inoculations or the volume of liquid (10 μl) injected. The mice inoculated with imiquimod developed, in addition to suppurative meningitis, moderate to severe suppurative ventriculitis, characterized by mild hemorrhage and infiltration of the lateral ventricles by neutrophils and lymphocytes (Fig. 4*A*). The suppurative ventriculitis was the only consistent pathological change associated with imiquimod inoculation and was not observed in mock- or LPS-treated animals (Fig. 4*B* and data not shown).

To examine cellular changes at the molecular level, we analyzed the mRNA expression of *Gfap*, which is up-regulated during astrocyte activation. Additionally, we analyzed mRNA expression of *F4/80*, a macrophage and microglia marker; Cd3ε polypeptide (*Cd3ε*), a marker for T cell infiltration; and *Icam-1*, which is up-regulated on peripheral endothelial cells following stimulation with TLR7 agonists (54). Administration of imiquimod induced *Gfap* and *Icam-1* mRNA expression at 12 hpi, but did not significantly alter the expression of either *F4/80* or *Cd3ε* mRNA at any of the time points analyzed (Fig. 5). In contrast, LPS administration induced prolonged up-regulation of *F4/80* mRNA to 96 hpi and increased expression of *Cd3ε* mRNA at 13 days after inoculation (days post infection; Fig. 5). Thus, stimulation of either TLR7 or TLR4 resulted in astrocyte activation and up-regulation of adhesion molecules, but only TLR4 stimulation induced mRNA up-regulation of the microglia/macrophage marker *F4/80*.

To better understand which cells in the CNS were responding to agonist administration, we analyzed tissue samples from mice at 12 hpi by in situ hybridization. We analyzed cells for *Ccl2* mRNA expression since this chemokine is often associated with viral infection in the CNS (45, 52). *Ccl2*-positive cells in imiquimod-treated mice were located at the edges of the ventricles and spread out into the tissue (Fig. 4*C*). Dual staining for GFAP expression

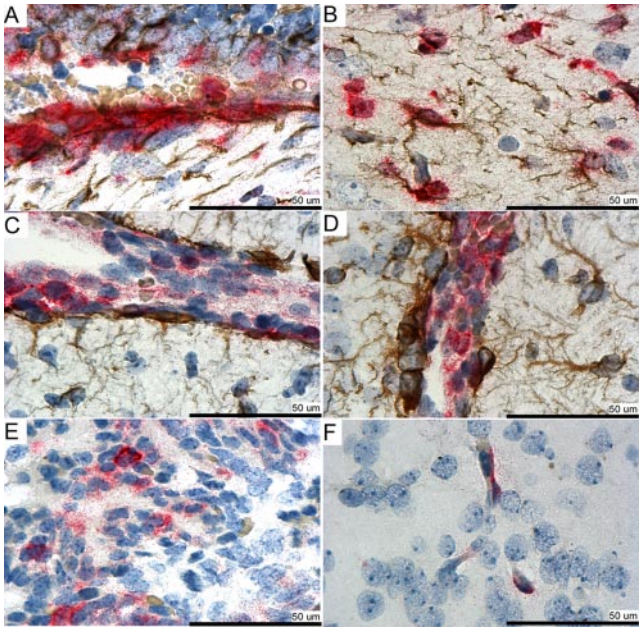

FIGURE 6. In situ hybridization-immunohistochemistry analysis of mid-coronal sections of imiquimod (*A*, *B*, *E*, and *F*)- and LPS-inoculated (*C* and *D*) neonatal brain. Tissue sections were stained as described for Fig. 3, *C–F*. *A* and *B,* GFAP-positive astrocytes (brown stain) express *Ccl2*-mRNA (red stain) in imiquimod-treated mice. Images are from the same region shown in Fig. 3, *A* and *C*. *C* and *D,* Infiltrating cells, not GFAP-positive astrocytes, express *Ccl2* mRNA in LPS-treated mice. Images are from the same region shown in Fig. 3, *B* and *D*. *E, Ccl2*-positive cells from choroid plexus include ependymal and epithelial cells. *F,* Capillary endothelial cells in thalamus are also positive for *Ccl2* mRNA expression in imiquimod-treated mice. All images were taken with a digital camera attached to an Olympus scope. Scale bars are shown for all images. Images are representative of cells in the surrounding area. Data are representative of two replicate experiments. Nonspecific RNA probes and no-primary Ab controls were used as controls for all experiments.

Table II. *Properties of TLR7 and TLR8 agonists used*

Ligand	Description	Stimulation of	
		Human TLR7	Human TLR8
Imiquimod (R837)	Imidazoquinoline	+	−
Loxoribine (7-allyl-8-oxoguanosine)	Guanosine analog	+	−
CL087	Adenine analog	+	−
3M002 (CL075)	Thiazoloquinoline	−	+
CL097	Imidazoquinoline	+	+

demonstrated that the *Ccl2*-positive cells lining the ventricles (Fig. 6*A*) as well as in the tissue (Fig. 6*B*) were primarily astrocytes. *Ccl2*-positive cells were also detected in the choroid plexus (Fig. 4*E*), with *Ccl2*-expressing ependymal cells and endothelia (Fig. 6*E* and data not shown) observed. Brain capillary endothelia located in the thalamus were also positive for *Ccl2* (Fig. 6*F*). Thus, multiple cell types respond to imiquimod stimulation including astrocytes, ependymal, and endothelial cells. In contrast, *Ccl2*-positive cells in LPS-treated mice appeared to be primarily infiltrating cells within the ventricles (Figs. 4, *D* and *F*, and 6*C*). Astrocytes were not positive for *Ccl2* mRNA in LPS-treated mice (Fig. 6*D*). Thus, despite the common up-regulation of *Ccl2* mRNA and protein by imiquimod and LPS, the cellular source of *Ccl2* at 12 h after infection was different between these two agonists.

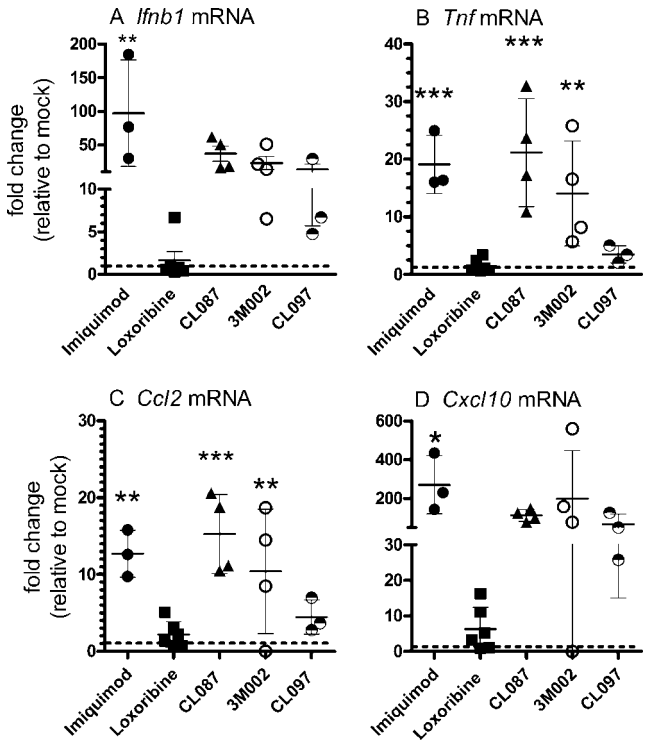

FIGURE 7. In vivo response to stimulation by various TLR7/8 agonists in the developing brain. One hundred nanomoles of the appropriate agonist was inoculated icv into 2-day-old mice as described in Fig. 1. At 12 hpi, brain tissue was removed and snap frozen in liquid nitrogen. Samples were analyzed as described in Fig. 1. Fold increase in *Ifnb1* (*A*), *Tnf* (*B*), *Ccl2* (*C*), and *Cxcl10* (*D*) mRNA as compared with mock-infected controls. Each symbol represents an individual animal for the group. Data are the mean ± SD for three to six mice per group and are representative of two replicate experiments. Statistical analysis was completed by one-way ANOVA with the Newman-Keuls post test. *, $p < 0.05$; **, $p < 0.01$; and ***, $p < 0.001$.

Comparison between TLR7/8 agonists

Recent studies have indicated that murine TLR8 is functional (55, 56) and that murine TLR8 can be stimulated on neurons (55, 56). Differences in the chemical structure were shown to influence binding of agonists to human TLR7 and human TLR8 (Table II) (35, 36). To investigate possible differences between these agonists in inducing neuroinflammation, we compared three TLR7 agonists (imiquimod, loxoribine, and CL087), a TLR8 agonist (3M002), and a TLR7/8 agonist (CL097) (Table II). Interestingly, the ability of these agonists to induce cytokine/chemokine responses was not divided between TLR7 or TLR8 stimulation capabilities. Two TLR7 agonists (imiquimod and CL087) and the TLR8 agonist (3M002) induced similar levels of proinflammatory cytokines and chemokines (Fig. 7). The TLR7/8 agonist, CL097, induced *Ifnb1* and *Cxcl10* mRNA expression, but did not induce the expression of *Tnf* or *Ccl2* mRNA. Loxoribine, a TLR7 agonist similar to imiquimod, induced only minimal expression of proinflammatory cytokines and chemokines compared with the other agonists. Thus, TLR7/TLR8 agonists differed in their ability to induce proinflammatory responses in the CNS in mice.

TLR7 contributes to both the imiquimod- and 3M002-induced response

3M002 stimulated human TLR8 or mouse TLR8- transfected HEK cells, but not human TLR7-transfected HEK cells (41). To investigate whether 3M002-induced neuroinflammation was mediated by TLR7 or TLR8, we used TLR7-deficient mice. As a control, we also analyzed imiquimod-induced neuroinflammatory responses in TLR7-sufficient and -deficient mice. Both imiquimod and 3M002 induced significant up-regulation of *Ifnb1, Tnf, Ccl2* (MCP-1), and *Cxcl10* (IP-10) mRNA levels in the brain of TLR7-sufficient (+ or +/−) mice at 12 hpi (Fig. 8). In contrast, imiquimod did not up-regulate any of the cytokines or chemokines in TLR7-deficient (−/− or −) mice. This confirms that imiquimod up-regulated the proinflammatory cytokines and chemokines in the brain through the TLR7 pathway, not through TLR8. 3M002-induced cytokine and chemokine expression was greatly reduced in TLR7-deficient compared with TLR7-sufficient mice (Fig. 8*B*). However, 3M002 did induce a low level of *Ccl2* and *Ifnb1* mRNA expression, indicating that 3M002 may also be stimulating through TLR8, albeit at a much lower level than TLR7 (Fig. 8*B*).

Astrocyte response differs between imiquimod and loxoribine

The difference between the abilities of imiqumod and loxoribine to induce cytokine and chemokine responses in vivo (Fig. 7) was surprising since both agonists stimulate TLR7 in dendritic cells and macrophages (35, 36, 42). Therefore, we compared the ability of these agonists to stimulate cells in vitro. Since astrocytes were one of the primary cell populations to respond to imiquimod stimulation, we examined the ability of imiquimod and loxoribine to stimulate the astrocyte cell line C8D1A. As a positive control, we

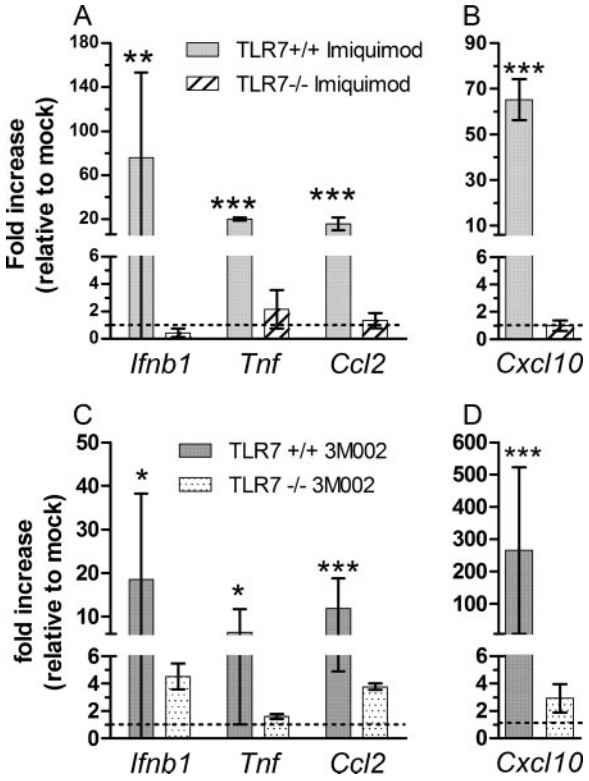

FIGURE 8. Influence of TLR7 deficiency on cytokine and chemokine mRNA expression following imiquimod (*A* and *B*) or 3M002 (*C* and *D*) inoculation. TLR7 wild-type/homozygous-positive (+/+, +) or heterozygous positive (+/−) or TLR7-deficient mice were inoculated as described Fig. 1. Brain tissues were removed at 12 hpi, processed, and analyzed as described in Fig. 1. Data are the mean ± SD for three to four mice per group and are representative of two replicate experiments. Statistical analysis was completed by one-way ANOVA with the Newman-Keuls post test. *, $p < 0.05$; **, $p < 0.01$; and ***, $p < 0.001$.

used the macrophage cell line RAW264.7. Both cell types express TLR7 as detected by intracellular flow cytometry staining (Fig. 9, *A* and *B*). Imiquimod stimulation of C8D1A cells induced high levels of *Tnf* mRNA (Fig. 9*C*). In contrast, only low levels of *Tnf* mRNA were expressed following loxoribine stimulation. As expected, both loxoribine and imiquimod induced up-regulation of *Tnf* mRNA expression in a macrophage cell line (Fig. 9*D*). Thus, the difference between the responses to imiquimod and loxoribine in vivo may be due to their abilities to activate certain cell types of the CNS, such as astrocytes.

Discussion

Although TLR7 is a known mediator of immune responses to ssRNA viruses, very little is known about the role of this receptor in neuroinflammation. In the present study, we demonstrated that a single inoculum of a TLR7 agonist was sufficient to induce a pronounced neuroinflammatory response, including the production of multiple proinflammatory cytokines and chemokines, as well as the activation of astrocytes. The duration of the response was limited as both cytokine and chemokine induction and astrocyte activation waned by 48 h after stimulation. Thus, TLR7 stimulation induced a short, but pronounced, neuroinflammatory response in the CNS and did not induce any obvious signs of distress. This contrasts with other TLR agonists such as LPS or CpG DNA which can induce neuronal apoptosis and/or animal death with a single icv administration (30, 57).

The neuroinflammatory responses induced by imiquimod stimulation in the brain were of short duration compared with LPS stimulation (Fig. 1). One possible reason for this is the anatomical location of these TLRs on the cells. TLR4 is located on the cell surface, whereas TLR7 is present within the cell on endosomal membranes. The polysaccharide side chains of LPS located on the bacterial surfaces can stimulate TLR4 located on the cell membranes directly. To stimulate TLR7 during viral infections, ssRNA must directly interact with the endosomal membranes either by direct uncoating in the endosomal membranes or by autophagy

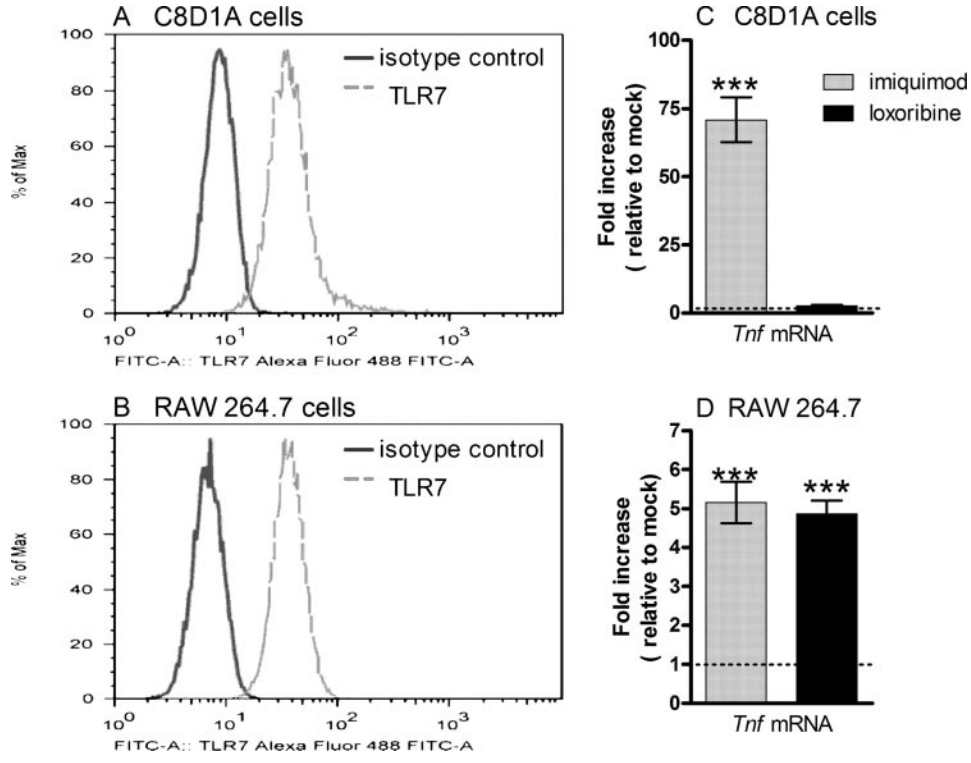

FIGURE 9. Expression of TLR7 on astrocytes (*A*; C8D1A) and macrophage cells (*B*; RAW) by intracellular flow cytometry analysis. Data were collected on a FACSAria and analyzed with FlowJo software. *Tnf* mRNA expression in C8DA1 (*C*) and RAW (*D*) cell cultures following stimulation with the TLR7 agonists imiquimod and loxoribine. Semiconfluent cultures of astrocytes or macrophages were stimulated with 100 μmol/ml imiquimod or loxoribine or mock stimulated. Cells were lysed at 48 h after stimulation and the RNA was isolated. Real-time quantitative RT-PCR analysis was performed using primers specific for *Tnf*, and *Gapdh* mRNA, and analyzed as described in Fig. 1. Data are the mean ± SD for three samples per group and represent one of three replicate experiments. Statistical analysis was completed by one-way ANOVA with the Newman-Keuls post test. ***, $p < 0.001$.

from the cytoplasm (58). This would limit the activation of cells to either infected cells or phagocytic cells surrounding the site of infection.

Another possible reason for the differences in neuroinflammatory responses induced by TLR7 and TLR4 agonists is that the structural complexity of the TLR7 agonists is quite different from that of the TLR4 agonists. The TLR4 agonist LPS is a large complex molecule consisting of lipids and polysaccharides. The TLR7 agonists used in the present study are small synthetic compounds which may be degraded rapidly. This may also be pertinent to the responses to bacterial vs viral infections, with bacterial LPS remaining stable and viral ssRNA being degraded by RNases. Thus, a robust viral infection with generation of substantial RNA particles may be needed to elicit an equivalent viral-mediated neuroinflammatory response. This is supported by observations of the inflammatory response to retrovirus infection in the CNS where peak chemokine mRNA expression correlated with peak viral RNA expression (45, 53, 59). Interestingly, the chemokine mRNA response started to decline at the approximate time when virus levels plateaued in the brain (45, 53, 59).

One of the primary differences in the response between imiquimod and LPS stimulation was the source of *Ccl2* mRNA (Figs. 4 and 6). In imiquimod-treated animals, the predominant cell type producing *Ccl2* mRNA was astrocytes, although not all astrocytes expressed *Ccl2* mRNA. CCL2 expression by astrocytes has been observed with virus infection, multiple sclerosis, and Alzheimer's disease (45, 60, 61). In contrast, astrocytes from LPS-stimulated animals were not positive for *Ccl2* mRNA (Figs. 4 and 6), although it is possible that these cells do express *Ccl2* mRNA at later time points following infection. However, the majority of the *Ccl2*-producing cells in the LPS-inoculated mice at 12 hpi were infiltrating cells, suggesting that most of the inflammatory response was also from infiltrating cells rather than the resident glial cells.

Dose curve analysis of imiquimod administration indicated that 100–200 nmol induced neuroinflammation, while 5-fold higher or lower concentrations did not. Possibly high concentrations of agonist overwhelm cells, resulting in the limitation of the production of proinflammatory cytokines and chemokines. Alternatively, at higher concentrations, individual agonists may aggregate, resulting in a diminished uptake by cells in the CNS.

In the current study, not all of the TLR7/8 agonists used induced neuroinflammatory responses. For example, the TLR7 agonist imiquimod induced astrocyte responses both in vivo and in vitro, whereas the TLR7 agonist loxoribine did not. In contrast, both imiquimod and loxoribine induced responses in macrophages, as have been reported for plasmacytoid dendritic cells and B cells (35, 36). These variations in neuroinflammatory responses among the TLR7/8 agonists used in the present study could be due to differential uptake of individual agonists by certain cell types. Possibly, loxoribine is not endocytosed by astrocytes as readily as imiquimod. It is also possible that astrocytes express other proteins in the endosome or on the cell surface that may preferentially bind loxoribine. Thus, a comparison between complementary agonists may be necessary to differentiate the functional responses to TLR7 or TLR8 in different cell types.

TLR7 and TLR8 are highly homologous and their distinct roles in innate immune responses are still being analyzed (36, 39). In our current study, the human TLR8 agonist 3M002 induced similar neuroinflammatory responses to the TLR7 agonists. However, this response appeared to be mediated primarily by TLR7, not TLR8. This agrees with in vitro studies in which 3M002 stimulation of human TLR8 but not mouse TLR8 induced NF-κB activation (41). Thus, in the mouse, 3M002 appears to stimulate primarily through TLR7 rather than TLR8.

TLR agonists are currently being studied as immune activators or immune response modifiers to enhance vaccines, improve the immune response to different cancers, and treat viral infections (62–65). In the present study, certain TLR7/8 agonists induced substantial proinflammatory responses in the CNS in terms of cellular activation and production of proinflammatory cytokines and chemokines, without inducing overt damage. This suggests that the TLR7/8 agonists may be used as immune response modifiers for diseases and conditions affecting the CNS provided they can cross the blood-brain barrier. These studies also demonstrate that TLR7/8 agonists can differ widely in their ability to induce neuroinflammation, as some of the agonists induced only minimal responses in the brain. Thus, agonists such as loxoribine may be effective in enhancing peripheral immune responses and yet limit the activation of glial cells and production of proinflammatory cytokines in the CNS. The differences between these immune response modifiers in inducing inflammatory responses may be beneficial when targeting a specific organ or cell type.

Acknowledgments

We thank Marilyn Dietrich for assistance with flow cytometry.

Disclosures

The authors have no financial conflict of interest.

References

1. Asensio, V. C., and I. L. Campbell. 1997. Chemokine gene expression in the brains of mice with lymphocytic choriomeningitis. *J. Virol.* 71: 7832–7840.
2. Dickson, D. W., J. F. Llena, S. J. Nelson, and K. M. Weidenheim. 1993. Central nervous system pathology in pediatric AIDS. *Ann. NY Acad. Sci.* 693: 93–106.
3. Griffin, D. E. 2003. Immune responses to RNA-virus infections of the CNS. *Nat. Rev. Immunol.* 3: 493–502.
4. Hunt, N. H., J. Golenser, T. Chan-Ling, S. Parekh, C. Rae, S. Potter, I. M. Medana, J. Miu, and H. J. Ball. 2006. Immunopathogenesis of cerebral malaria. *Int. J. Parasitol.* 36: 569–582.
5. Kelder, W., J. C. McArthur, T. Nance-Sproson, D. McClernon, and D. E. Griffin. 1998. β-Chemokines MCP-1 and RANTES are selectively increased in cerebrospinal fluid of patients with human immunodeficiency virus-associated dementia. *Ann. Neurol.* 44: 831–835.
6. McCoig, C., M. M. Castrejon, J. Saavedra-Lozano, E. Castano, C. Baez, E. R. Lanier, X. Saez-Llorens, and O. Ramilo. 2004. Cerebrospinal fluid and plasma concentrations of proinflammatory mediators in human immunodeficiency virus-infected children. *Pediatr. Infect. Dis. J.* 23: 114–118.
7. Nau, R., and W. Bruck. 2002. Neuronal injury in bacterial meningitis: mechanisms and implications for therapy. *Trends Neurosci.* 25: 38–45.
8. Szklarczyk, A., M. Stins, E. A. Milward, H. Ryu, C. Fitzsimmons, D. Sullivan, and K. Conant. 2007. Glial activation and matrix metalloproteinase release in cerebral malaria. *J. Neurovirol.* 13: 2–10.
9. Wilson, E. H., and C. A. Hunter. 2004. The role of astrocytes in the immunopathogenesis of toxoplasmic encephalitis. *Int. J. Parasitol.* 34: 543–548.
10. Vargas, D. L., C. Nascimbene, C. Krishnan, A. W. Zimmerman, and C. A. Pardo. 2005. Neuroglial activation and neuroinflammation in the brain of patients with autism. *Ann. Neurol.* 57: 67–81.
11. Sun, Y. X., L. Minthon, A. Wallmark, S. Warkentin, K. Blennow, and S. Janciauskiene. 2003. Inflammatory markers in matched plasma and cerebrospinal fluid from patients with Alzheimer's disease. *Dement. Geriatr. Cogn. Disord.* 16: 136–144.
12. Konsman, J. P., B. Drukarch, and A. M. Van Dam. 2007. (Peri)vascular production and action of pro-inflammatory cytokines in brain pathology. *Clin. Sci.* 112: 1–25.
13. Cohly, H. H., and A. Panja. 2005. Immunological findings in autism. *Int. Rev. Neurobiol.* 71: 317–341.
14. Ahlsen, G., L. Rosengren, M. Belfrage, A. Palm, K. Haglid, A. Hamberger, and C. Gillberg. 1993. Glial fibrillary acidic protein in the cerebrospinal fluid of children with autism and other neuropsychiatric disorders. *Biol. Psychiatry* 33: 734–743.
15. Dickson, D. W., S. C. Lee, L. A. Mattiace, S. H. Yen, and C. Brosnan. 1993. Microglia and cytokines in neurological disease, with special reference to AIDS and Alzheimer's disease. *Glia* 7: 75–83.
16. Hornig, M., and W. I. Lipkin. 2001. Infectious and immune factors in the pathogenesis of neurodevelopmental disorders: epidemiology, hypotheses, and animal models. *Ment. Retard. Dev. Disabil. Res. Rev.* 7: 200–210.
17. Hornig, M., R. Mervis, K. Hoffman, and W. I. Lipkin. 2002. Infectious and immune factors in neurodevelopmental damage. *Mol. Psychiatry* 7 (*Suppl.* 2): S34–S35.

18. Minagar, A., P. Shapshak, R. Fujimura, R. Ownby, M. Heyes, and C. Eisdorfer. 2002. The role of macrophage/microglia and astrocytes in the pathogenesis of three neurologic disorders: HIV-associated dementia, Alzheimer disease, and multiple sclerosis. *J. Neurol. Sci.* 202: 13–23.
19. Akira, S., K. Takeda, and T. Kaisho. 2001. Toll-like receptors: critical proteins linking innate and acquired immunity. *Nat. Immunol.* 2: 675–680.
20. Janeway, C. A., Jr. 1992. The immune system evolved to discriminate infectious nonself from noninfectious self. *Immunol. Today* 13: 11–16.
21. Medzhitov, R., and C. A. Janeway, Jr. 1997. Innate immunity: the virtues of a nonclonal system of recognition. *Cell* 91: 295–298.
22. Kaisho, T., and S. Akira. 2006. Toll-like receptor function and signaling. *J. Allergy Clin. Immunol.* 117: 979–987.
23. McKimmie, C. S., N. Johnson, A. R. Fooks, and J. K. Fazakerley. 2005. Viruses selectively upregulate Toll-like receptors in the central nervous system. *Biochem. Biophys. Res. Commun.* 336: 925–933.
24. McKimmie, C. S., and J. K. Fazakerley. 2005. In response to pathogens, glial cells dynamically and differentially regulate Toll-like receptor gene expression. *J. Neuroimmunol.* 169: 116–125.
25. Mishra, B. B., P. K. Mishra, and J. M. Teale. 2006. Expression and distribution of Toll-like receptors in the brain during murine neurocysticercosis. *J. Neuroimmunol.* 181: 46–56.
26. Aravalli, R. N., P. K. Peterson, and J. R. Lokensgard. 2007. Toll-like receptors in defense and damage of the central nervous system. *J. Neuroimmune Pharmacol.* 2: 297–312.
27. Dalpke, A. H., M. K. Schafer, M. Frey, S. Zimmermann, J. Tebbe, E. Weihe, and K. Heeg. 2002. Immunostimulatory CpG-DNA activates murine microglia. *J. Immunol.* 168: 4854–4863.
28. Iliev, A. I., A. K. Stringaris, R. Nau, and H. Neumann. 2004. Neuronal injury mediated via stimulation of microglial Toll-like receptor-9 (TLR9). *FASEB J.* 18: 412–414.
29. Kurt-Jones, E. A., M. Chan, S. Zhou, J. Wang, G. Reed, R. Bronson, M. M. Arnold, D. M. Knipe, and R. W. Finberg. 2004. Herpes simplex virus 1 interaction with Toll-like receptor 2 contributes to lethal encephalitis. *Proc. Natl. Acad. Sci. USA* 101: 1315–1320.
30. Pedras-Vasconcelos, J. A., D. Goucher, M. Puig, L. H. Tonelli, V. Wang, S. Ito, and D. Verthelyi. 2006. CpG oligodeoxynucleotides protect newborn mice from a lethal challenge with the neurotropic Tacaribe arenavirus. *J. Immunol.* 176: 4940–4949.
31. Wang, T., T. Town, L. Alexopoulou, J. F. Anderson, E. Fikrig, and R. A. Flavell. 2004. Toll-like receptor 3 mediates West Nile virus entry into the brain causing lethal encephalitis. *Nat. Med.* 10: 1366–1373.
32. Zhang, S. Y., E. Jouanguy, S. Ugolini, A. Smahi, G. Elain, P. Romero, D. Segal, V. Sancho-Shimizu, L. Lorenzo, A. Puel, et al. 2007. TLR3 deficiency in patients with herpes simplex encephalitis. *Science* 317: 1522–1527.
33. Aravalli, R. N., S. Hu, T. N. Rowen, J. M. Palmquist, and J. R. Lokensgard. 2005. Cutting edge: TLR2-mediated proinflammatory cytokine and chemokine production by microglial cells in response to herpes simplex virus. *J. Immunol.* 175: 4189–4193.
34. Xia, Y., K. Yamagata, and T. L. Krukoff. 2006. Differential expression of the CD14/TLR4 complex and inflammatory signaling molecules following i.c.v. administration of LPS. *Brain Res.* 1095: 85–95.
35. Hemmi, H., T. Kaisho, O. Takeuchi, S. Sato, H. Sanjo, K. Hoshino, T. Horiuchi, H. Tomizawa, K. Takeda, and S. Akira. 2002. Small anti-viral compounds activate immune cells via the TLR7 MyD88-dependent signaling pathway. *Nat. Immunol.* 3: 196–200.
36. Lee, J., T. H. Chuang, V. Redecke, L. She, P. M. Pitha, D. A. Carson, E. Raz, and H. B. Cottam. 2003. Molecular basis for the immunostimulatory activity of guanine nucleoside analogs: activation of Toll-like receptor 7. *Proc. Natl. Acad. Sci. USA* 100: 6646–6651.
37. Diebold, S. S., T. Kaisho, H. Hemmi, S. Akira, and C. Reis e Sousa. 2004. Innate antiviral responses by means of TLR7-mediated recognition of single-stranded RNA. *Science* 303: 1529–1531.
38. Lund, J. M., L. Alexopoulou, A. Sato, M. Karow, N. C. Adams, N. W. Gale, A. Iwasaki, and R. A. Flavell. 2004. Recognition of single-stranded RNA viruses by Toll-like receptor 7. *Proc. Natl. Acad. Sci. USA* 101: 5598–5603.
39. Heil, F., H. Hemmi, H. Hochrein, F. Ampenberger, C. Kirschning, S. Akira, G. Lipford, H. Wagner, and S. Bauer. 2004. Species-specific recognition of single-stranded RNA via Toll-like receptor 7 and 8. *Science* 303: 1526–1529.
40. Ma, Y., J. Li, I. Chiu, Y. Wang, J. A. Sloane, J. Lu, B. Kosaras, R. L. Sidman, J. J. Volpe, and T. Vartanian. 2006. Toll-like receptor 8 functions as a negative regulator of neurite outgrowth and inducer of neuronal apoptosis. *J. Cell Biol.* 175: 209–215.
41. Gorden, K. B., K. S. Gorski, S. J. Gibson, R. M. Kedl, W. C. Kieper, X. Qiu, M. A. Tomai, S. S. Alkan, and J. P. Vasilakos. 2005. Synthetic TLR agonists reveal functional differences between human TLR7 and TLR8. *J. Immunol.* 174: 1259–1268.
42. Heil, F., P. Ahmad-Nejad, H. Hemmi, H. Hochrein, F. Ampenberger, T. Gellert, H. Dietrich, G. Lipford, K. Takeda, S. Akira, et al. 2003. The Toll-like receptor 7 (TLR7)-specific stimulus loxoribine uncovers a strong relationship within the TLR7, 8 and 9 subfamily. *Eur. J. Immunol.* 33: 2987–2997.
43. Lee, J., C. C. Wu, K. J. Lee, T. H. Chuang, K. Katakura, Y. T. Liu, M. Chan, R. Tawatao, M. Chung, C. Shen, et al. 2006. Activation of anti-hepatitis C virus responses via Toll-like receptor 7. *Proc. Natl. Acad. Sci. USA* 103: 1828–1833.
44. Wille-Reece, U., B. J. Flynn, K. Lore, R. A. Koup, A. P. Miles, A. Saul, R. M. Kedl, J. J. Mattapallil, W. R. Weiss, M. Roederer, and R. A. Seder. 2006. Toll-like receptor agonists influence the magnitude and quality of memory T cell responses after prime-boost immunization in nonhuman primates. *J. Exp. Med.* 203: 1249–1258.
45. Peterson, K. E., J. S. Errett, T. Wei, D. E. Dimcheff, R. Ransohoff, W. A. Kuziel, L. Evans, and B. Chesebro. 2004. MCP-1 and CCR2 contribute to non-lymphocyte-mediated brain disease induced by Fr98 polytropic retrovirus infection in mice: role for astrocytes in retroviral neuropathogenesis. *J. Virol.* 78: 6449–6458.
46. Poulsen, D. J., C. Favara, E. Y. Snyder, J. Portis, and B. Chesebro. 1999. Increased neurovirulence of polytropic mouse retroviruses delivered by inoculation of brain with infected neural stem cells. *Virology* 263: 23–29.
47. Rozen, S., and H. J. Skaletsky. 2000. *Primer3 on the WWW for General Users and for Biologist Programmers.* S. Krawetz and S. Misener, eds. Humana, Ckifton, NJ, pp. 365–386.
48. Perlman, J. M., and C. Argyle. 1992. Lethal cytomegalovirus infection in preterm infants: clinical, radiological, and neuropathological findings. *Ann. Neurol.* 31: 64–68.
49. Clancy, B., R. B. Darlington, and B. L. Finlay. 2001. Translating developmental time across mammalian species. *Neuroscience* 105: 7–17.
50. Cunningham, C., D. C. Wilcockson, S. Campion, K. Lunnon, and V. H. Perry. 2005. Central and systemic endotoxin challenges exacerbate the local inflammatory response and increase neuronal death during chronic neurodegeneration. *J. Neurosci.* 25: 9275–9284.
51. Kerr, J. R., F. Barah, M. L. Chiswick, G. V. McDonnell, J. Smith, M. D. Chapman, J. B. Bingham, P. Kelleher, and M. N. Sheppard. 2002. Evidence for the role of demyelination, HLA-DR alleles, and cytokines in the pathogenesis of parvovirus B19 meningoencephalitis and its sequelae. *J. Neurol. Neurosurg. Psychiatry* 73: 739–746.
52. McManus, C. M., K. Weidenheim, S. E. Woodman, J. Nunez, J. Hesselgesser, A. Nath, and J. W. Berman. 2000. Chemokine and chemokine-receptor expression in human glial elements: induction by the HIV protein, Tat, and chemokine autoregulation. *Am. J. Pathol.* 156: 1441–1453.
53. Peterson, K. E., S. J. Robertson, J. L. Portis, and B. Chesebro. 2001. Differences in cytokine and chemokine responses during neurological disease induced by polytropic murine retroviruses map to separate regions of the viral envelope gene. *J. Virol.* 75: 2848–2856.
54. Gunzer, M., H. Riemann, Y. Basoglu, A. Hillmer, C. Weishaupt, S. Balkow, B. Benninghoff, B. Ernst, M. Steinert, T. Scholzen, et al. 2005. Systemic administration of a TLR7 ligand leads to transient immune incompetence due to peripheral-blood leukocyte depletion. *Blood* 106: 2424–2432.
55. Gorden, K. K., X. Qiu, J. J. Battiste, P. P. Wightman, J. P. Vasilakos, and S. S. Alkan. 2006. Oligodeoxynucleotides differentially modulate activation of TLR7 and TLR8 by imidazoquinolines. *J. Immunol.* 177: 8164–8170.
56. Gorden, K. K., X. X. Qiu, C. C. Binsfeld, J. P. Vasilakos, and S. S. Alkan. 2006. Cutting edge: activation of murine TLR8 by a combination of imidazoquinoline immune response modifiers and poly(T) oligodeoxynucleotides. *J. Immunol.* 177: 6584–6587.
57. Macagno, A., M. Molteni, A. Rinaldi, F. Bertoni, A. Lanzavecchia, C. Rossetti, and F. Sallusto. 2006. A cyanobacterial LPS antagonist prevents endotoxin shock and blocks sustained TLR4 stimulation required for cytokine expression. *J. Exp. Med.* 203: 1481–1492.
58. Lee, H. K., J. M. Lund, B. Ramanathan, N. Mizushima, and A. Iwasaki. 2007. Autophagy-dependent viral recognition by plasmacytoid dendritic cell. *Science* 315: 1398–1401.
59. Peterson, K. E., L. H. Evans, K. Wehrly, and B. Chesebro. 2006. Increased proinflammatory cytokine and chemokine responses and microglial infection following inoculation with neural stem cells infected with polytropic murine retroviruses. *Virology* 354: 143–153.
60. Johnstone, M., A. J. Gearing, and K. M. Miller. 1999. A central role for astrocytes in the inflammatory response to β-amyloid; chemokines, cytokines, and reactive oxygen species are produced. *J. Neuroimmunol.* 93: 182–193.
61. McManus, C., J. W. Berman, F. M. Brett, H. Staunton, M. Farrell, and C. F. Brosnan. 1998. MCP-1, MCP-2, and MCP-3 expression in multiple sclerosis lesions: an immunohistochemical and in situ hybridization study. *J. Neuroimmunol.* 86: 20–29.
62. Wang, Y., K. Abel, K. Lantz, A. M. Krieg, M. B. McChesney, and C. J. Miller. 2005. The Toll-like receptor 7 (TLR7) agonist, imiquimod, and the TLR9 agonist, CpG ODN, induce antiviral cytokines and chemokines but do not prevent vaginal transmission of simian immunodeficiency virus when applied intravaginally to rhesus macaques. *J. Virol.* 79: 14355–14370.
63. Murad, Y. M., T. M. Clay, H. K. Lyerly, and M. A. Morse. 2007. CPG-7909 (PF-3512676, ProMune): Toll-like receptor-9 agonist in cancer therapy. *Expert. Opin. Biol. Ther.* 7: 1257–1266.
64. Zaks, K., M. Jordan, A. Guth, K. Sellins, R. Kedl, A. Izzo, C. Bosio, and S. Dow. 2006. Efficient immunization and cross-priming by vaccine adjuvants containing TLR3 or TLR9 agonists complexed to cationic liposomes. *J. Immunol.* 176: 7335–7345.
65. Wille-Reece, U., B. J. Flynn, K. Lore, R. A. Koup, R. M. Kedl, J. J. Mattapallil, W. R. Weiss, M. Roederer, and R. A. Seder. 2005. HIV Gag protein conjugated to a Toll-like receptor 7/8 agonist improves the magnitude and quality of Th1 and $CD8^+$ T cell responses in nonhuman primates. *Proc. Natl. Acad. Sci. USA* 102: 15190–15194.